

# Phonon heat conduction in a semiconductor nanowire

Jie Zou<sup>a)</sup> and Alexander Balandin

*Department of Electrical Engineering, University of California at Riverside, Riverside, California 92521*

(Received 23 October 2000; accepted for publication 4 December 2000)

A model for phonon heat conduction in a semiconductor nanowire with dimensions comparable to the phonon mean free path is developed. It is based on the solution of Boltzmann's equation, which takes into account (i) modification of the acoustic phonon dispersion due to spatial confinement, and (ii) change in the nonequilibrium phonon distribution due to partially diffuse boundary scattering. Numerical simulation is performed for a silicon nanowire with boundaries characterized by different interface roughness. Phonon confinement and boundary scattering lead to a significant decrease of the lattice thermal conductivity. The value of this decrease and its interface roughness and temperature dependence are different from the predictions of the early models. The observed change in thermal resistance has to be taken into account in simulation of deep-submicron and nanometer-scale devices. © 2001 American Institute of Physics. [DOI: 10.1063/1.1345515]

## I. INTRODUCTION

As the transistor counts on the high-end microprocessor vanguard rush toward the 200 million mark and the feature dimensions shrink toward nanometer scale, thermal properties of semiconductor nanostructures are beginning to attract significant attention.<sup>1–3</sup> Several major factors explain recent interest to investigation of thermal conductivity in quantum confined structures. The most important one is a continuous scaling down of the feature sizes in electronic devices and circuits, which leads to an increase in power dissipation per unit area despite the reduction of the power supply voltage.<sup>4</sup> In addition, a variety of size effects that manifest themselves at nanoscale are extremely interesting from the physics point of view.

In this article we investigate phonon heat conduction in a generic semiconductor nanowire with lateral dimensions comparable to the acoustic phonon mean free path (MFP). The latter is 41 nm in the Debye model at room temperature, and 260 nm in the kinetic theory with dispersion.<sup>1</sup> We refer to our structure as a nanowire rather than a quantum wire to emphasize that the size effects, which modify phonon transport, may occur in structures with a larger feature size (hundreds of nanometers) than that required for carrier quantum confinement effects to take place. At the same time, our model is applicable to a very narrow quantum wire, where carrier transport is confined, as long as lateral dimensions of the wire are much larger than the lattice constant of the material ( $a=0.543$  nm for silicon at room temperature). These quasio-one-dimensional (1D) structures have recently been proposed for applications in quantum wire transistors,<sup>5</sup> quantum wire lasers,<sup>6</sup> and thermoelectric quantum wire arrays.<sup>7</sup> It can also be viewed as an ultimate narrow channel of a scaled down conventional metal–oxide–semiconductor field-effect transistor. The development of sophisticated patterning and self-assembly techniques now allows fabrication of high quality nanowires. Recently, it has been shown experimen-

tally that electrical conductivity of silicon nanowires 15–35 nm in diameter can be varied by as much as four orders of magnitude by doping and thermal treatment.<sup>8</sup> Nanowires with widths down to 10 nm and small size fluctuations have been fabricated by regular electron beam lithography and wet etching.<sup>9</sup>

To date, there have been three distinctively different approaches proposed for calculating the lattice thermal conductivity in nanowires (quantum wires). The first approach is based on the effectively bulk formulae for the lattice thermal conductivity but includes modification of acoustic phonon dispersion and group velocity in a nanowire due to phonon confinement effects.<sup>10,11</sup> The latter allowed the authors to introduce size effects beyond regular phonon-boundary scattering. However, this approach does not consider the modification of nonequilibrium phonon distribution due to boundary scattering. We call this approach A1 in the rest of the article. The second approach, on the contrary, corrects the formula for thermal conductivity by solving the linearized Boltzmann equation with given boundary conditions but uses bulk acoustic phonon dispersion and phonon MFP.<sup>12</sup> The latter neglects effects of acoustic phonon confinement, which become significant as the structure size approaches the phonon MFP. This approach is referred to as A2. The third approach deals with a specific case of very narrow quantum wires and solves the problem using the molecular dynamics method.<sup>13</sup> This method allows accurate calculation of phonon dispersion and thermal conductivity of structures with a few atomic layers but it does not allow us to include a variety of quantum effects, requires knowledge of interatomic potential, and is limited by the computation time.

In this article we propose a model that combines the first two approaches (denoted by A1+A2) and presents a more consistent way of calculating the lattice thermal conductivity in quasi-1D nanostructures. The presented model does not use the assumption of the constant phonon relaxation time but calculates it from the first principles. We generalize our model to include phonon relaxation on free electrons, which is important for scaled down device channels. The effects of

<sup>a)</sup>Electronic mail: jzou@ee.ucr.edu

interface quality characterized by the ratio between specular and diffuse phonon-boundary scattering is also analyzed. The rest of the article is organized as follows. In the next section, we present the theory. Results of numerical simulations and discussion are given in Sec. III. Our conclusions are presented in Sec. IV.

## II. THEORY

### A. Phonon Boltzmann equation

A phonon of energy  $\hbar\omega_s(\mathbf{q})$  and velocity  $\mathbf{V}_s(\mathbf{q})$  in the direction of  $\mathbf{q}$  contributes  $\hbar\omega_s(\mathbf{q})\mathbf{V}_s(\mathbf{q})$  to the heat current. The net phonon heat current with a small temperature gradient  $\nabla T$  is given by

$$\mathbf{J}_Q = - \sum_{\mathbf{q},s} \tilde{N}_{\mathbf{q},s} \hbar\omega_s(\mathbf{q}) \mathbf{V}_s(\mathbf{q}), \quad (1)$$

where subscript  $s$  refers to a particular phonon polarization type,  $\mathbf{q}$  is the phonon wavevector,  $\hbar$  is the Planck constant,  $\omega$  is the phonon frequency,  $\mathbf{V}_s(\mathbf{q})$  is the phonon group velocity, and  $\tilde{N}_{\mathbf{q},s} \equiv N_{\mathbf{q},s}^0 - N_{\mathbf{q},s}$  is the deviation of the phonon distribution,  $N_{\mathbf{q},s}$ , from its equilibrium value,  $N_{\mathbf{q},s}^0$ . The equilibrium phonon distribution,  $N_{\mathbf{q},s}^0$ , is given by the Bose–Einstein distribution

$$N_{\mathbf{q},s}^0 = \frac{1}{\exp(\hbar\omega_s(\mathbf{q})/k_B T) - 1}. \quad (2)$$

By definition

$$\mathbf{J}_Q = -\kappa_l \nabla T. \quad (3)$$

Thus, the problem of determining the lattice thermal conductivity is essentially that of obtaining  $\tilde{N}_{\mathbf{q},s}$ . In order to do this we need to solve the Boltzmann equation for  $\tilde{N}_{\mathbf{q},s}$ . In steady state, the phonon Boltzmann equation can be written as

$$\left( \frac{\partial N_{\mathbf{q},s}}{\partial t} \right)_{\text{drift}} + \left( \frac{\partial N_{\mathbf{q},s}}{\partial t} \right)_{\text{scatt}} = 0. \quad (4)$$

In Eq. (4),  $(\partial N_{\mathbf{q},s}/\partial t)_{\text{drift}}$  represents the change of the phonon distribution in the presence of a temperature gradient, and it is given by

$$\left( \frac{\partial N_{\mathbf{q},s}}{\partial t} \right)_{\text{drift}} = -\mathbf{V}_s(\mathbf{q}) \cdot \nabla N_{\mathbf{q},s} = -(\mathbf{V}_s(\mathbf{q}) \cdot \nabla T) \frac{\partial N_{\mathbf{q},s}}{\partial T}. \quad (5)$$

The value of  $N_{\mathbf{q},s}$  may also change due to scattering by other phonons, impurities, charge carriers, interfaces, boundaries, etc. The change in  $N_{\mathbf{q},s}$  due to these processes is denoted in Eq. (4) by  $(\partial N_{\mathbf{q},s}/\partial t)_{\text{scatt}}$ . In the relaxation-time approximation this term can be written as

$$\left( \frac{\partial N_{\mathbf{q},s}}{\partial t} \right)_{\text{scatt}} = \frac{N_{\mathbf{q},s}^0 - N_{\mathbf{q},s}}{\tau_{Cs}(\mathbf{q})}, \quad (6)$$

where  $\tau_{Cs}(\mathbf{q})$  is the combined phonon relaxation time. Substituting Eqs. (5) and (6) in (4), we can rewrite the phonon Boltzmann equation as

$$-V_x \frac{\partial N_{\mathbf{q},s}}{\partial x} - V_y \frac{\partial N_{\mathbf{q},s}}{\partial y} - V_z \frac{\partial N_{\mathbf{q},s}}{\partial z} + \frac{\tilde{N}_{\mathbf{q},s}}{\tau_{Cs}(\mathbf{q})} = 0, \quad (7)$$

where  $V_x$ ,  $V_y$ , and  $V_z$  are the three components of phonon group velocity along the  $x$ ,  $y$ , and  $z$  axis, respectively.

In our theoretical analysis, we consider a generic cylindrical quantum wire of diameter  $D$  with an axis along the  $z$  direction, and assume a temperature gradient along this axis. Eq. (7) then becomes

$$V_x \frac{\partial \tilde{N}_{\mathbf{q},s}}{\partial x} + V_y \frac{\partial \tilde{N}_{\mathbf{q},s}}{\partial y} + \frac{\tilde{N}_{\mathbf{q},s}}{\tau_{Cs}(\mathbf{q})} = V_z \frac{\partial T}{\partial z} \frac{\partial N_{\mathbf{q},s}}{\partial T}. \quad (8)$$

Assuming that the phonon distribution does not deviate strongly from its equilibrium value due to the temperature gradient, we can replace  $(\partial N_{\mathbf{q},s}/\partial T)$  by  $(\partial N_{\mathbf{q},s}^0/\partial T)$  in the right-hand side of the Eq. (8). This is a standard step used for solving such an equation. Correspondingly, the linearized phonon Boltzmann equation takes the form

$$V_x \frac{\partial \tilde{N}_{\mathbf{q},s}}{\partial x} + V_y \frac{\partial \tilde{N}_{\mathbf{q},s}}{\partial y} + \frac{\tilde{N}_{\mathbf{q},s}}{\tau_{Cs}(\mathbf{q})} = V_z \frac{\partial T}{\partial z} \frac{\partial N_{\mathbf{q},s}^0}{\partial T}. \quad (9)$$

In the subsection B, we introduce the expression for the lattice thermal conductivity in a nanowire in the spirit of the approach A2. It is based on the solution of Eq. (9) with appropriate boundary conditions.

### B. Calculation of the lattice thermal conductivity

For simplicity, we omit the subscripts  $\mathbf{q}$  and  $s$  in the rest of the article. In the bulk, the solution for Eq. (9) can be written as

$$\tilde{N} = \frac{\partial N^0}{\partial T} \nabla T \cdot \mathbf{V} \tau_C. \quad (10)$$

In the coordinate system that we have defined, we can further write  $\tilde{N}$  as

$$\tilde{N} = \frac{\partial N^0}{\partial T} \frac{\partial T}{\partial z} V_z \tau_C. \quad (11)$$

Substituting Eqs. (2) and (11) in Eq. (1) and comparing the result with Eq. (3), we obtain the regular bulk formula for the lattice thermal conductivity

$$\kappa_l = \left( \frac{k_B}{\hbar} \right)^3 \frac{k_B}{2\pi^2 V} T^3 \int_0^{\theta_D/T} \frac{\tau_C x^4 e^x}{(e^x - 1)^2} dx. \quad (12)$$

This equation is Klemens–Callaway’s expression for the lattice thermal conductivity in bulk, where  $k_B$  is the Boltzmann constant,  $\hbar$  is the Planck constant,  $V$  is the phonon group velocity,  $T$  is temperature,  $\theta_D$  is the Debye temperature,  $\tau_C$  is the combined phonon relaxation time, and  $x = \hbar\omega/k_B T$ . This equation has been used in the approach A1 with an appropriate modification of the phonon group velocity,  $V$ , and combined relaxation time,  $\tau_C$ , in a quantum well<sup>10</sup> and a quantum wire.<sup>11</sup>

We now introduce the parameter  $p$ , which characterizes the interface roughness and its effect on the phonon-boundary scattering.<sup>1</sup> The value of  $p$  represents the probability that the phonon is undergoing a specular scattering event at the interface. The value of  $1-p$  represents the probability that the phonon is undergoing a diffuse scattering event. One can also view  $p$  as the fraction of all phonons specularly

scattered from the boundary. In the case of purely specular interface scattering,  $p=1$ , the boundary condition on the Boltzmann equation is<sup>12</sup>

$$\tilde{N}(r=D/2; V_r) = \tilde{N}(r=D/2; -V_r), \tag{13}$$

where  $r = \sqrt{x^2 + y^2}$ , and  $V_r = \sqrt{V_x^2 + V_y^2}$ . In the case of purely diffuse scattering,  $p=0$ , the corresponding boundary condition is

$$\tilde{N}(r=D/2; -|V_r|) = 0. \tag{14}$$

In the case of purely specular scattering, which conserves crystal momentum,  $\tilde{N}$  does not change from its bulk value. In the case of diffuse or partially diffuse scattering, which is a resistive process,  $\tilde{N}$  deviates from its bulk value. The diffusive boundary scattering means that phonons can scatter from the interface at any direction irrespective of the angle of the incident phonon. In practice, the value of the  $p$  parameter is defined by the interface surface roughness. Following the derivation of Ref. 12, we solve Eq. (9) for  $\tilde{N}$  subject to the boundary conditions (13) and (14). The obtained lattice thermal conductivity of a nanowire,  $\kappa_l^{\text{wire}}$ , can be expressed via the bulk thermal conductivity,  $\kappa_l$ , and its deviation due to the phonon redistribution by the boundaries,  $\Delta\kappa_l^{\text{wire}}$ , as

$$\kappa_l^{\text{wire}}(T, p) = \kappa_l(T, p) - \Delta\kappa_l^{\text{wire}}(T, p). \tag{15}$$

The deviation in the thermal conductivity value,  $\Delta\kappa_l^{\text{wire}}$ , is given as

$$\Delta\kappa_l^{\text{wire}} = \frac{24}{\pi} \left(\frac{k_B}{\hbar}\right)^3 \frac{k_B}{2\pi^2 V} T^3 \int_0^{\theta_D/T} \frac{\tau_C x^4 e^x}{(e^x - 1)^2} G(\eta(x), p) dx, \tag{16}$$

where  $\eta$  is the ratio between the wire diameter  $D$  and the phonon mean free path  $\Lambda$ , i.e.,

$$\eta(x) = \frac{D}{\Lambda(x)}, \text{ with } \Lambda(x) = V(x) \tau_C(x). \tag{17}$$

Function  $G$  is given by

$$G(\eta(x), p) = (1-p)^2 \sum_{j=1}^{\infty} j p^{j-1} \int_0^1 (1-y^2)^{1/2} S_4(j\eta y) dy, \tag{18}$$

where

$$S_n(u) = \int_0^{\pi/2} e^{-u/\sin\theta} \cos^2\theta \sin^{n-3}\theta d\theta. \tag{19}$$

Substituting Eqs. (16)–(19) in Eq. (15) and using Eq. (12), we can further simplify the expression for  $\kappa_l^{\text{wire}}$  as

$$\begin{aligned} \kappa_l^{\text{wire}}(T, p) &= \left(\frac{k_B}{\hbar}\right)^3 \frac{k_B}{2\pi^2 V} T^3 \int_0^{\theta_D/T} \frac{\tau_C x^4 e^x}{(e^x - 1)^2} \\ &\quad \times \left[1 - \frac{24}{\pi} G(\eta(x), p)\right] dx. \end{aligned} \tag{20}$$

Analyzing Eqs. (16)–(20), we notice that when  $p \rightarrow 1$ ,  $G \rightarrow 0$ , and the deviation from the bulk formula disappears, i.e.,  $\Delta\kappa_l^{\text{wire}} = 0$  for all  $D$  in the case of purely specular scattering. However, the latter does not mean that the value of the thermal conductivity does not differ from its bulk value. Since the phonon dispersion and group velocity are different in a

nanowire, the phonon heat conduction is also changed. One should point out here that in the approach A2 the difference between a nanowire and bulk completely disappears at  $p = 1$ .<sup>12</sup> The phonon group velocity enters the expression of Eq. (20) for  $\kappa_l^{\text{wire}}(T, p)$  directly as well as via the expression for phonon scattering rates, which will be described below. When  $p \rightarrow 0$ , only the first term in the summation of Eq. (18) remains. When  $D \rightarrow \infty$ , the exponential term in Eq. (19) goes to zero leaving  $\Delta\kappa_l^{\text{wire}} = 0$  for all  $0 \leq p \leq 1$ .

### C. Phonon relaxation rates

In our model, we consider acoustic phonon relaxation in resistive processes, such as three-phonon Umklapp scattering, mass-difference scattering, boundary scattering, and phonon-electron scattering. The combined phonon relaxation time can be obtained by the summation of the inverse relaxation times for these scattering processes and in our case it is given as

$$\frac{1}{\tau_C} = \frac{1}{\tau_U} + \frac{1}{\tau_M} + \frac{1}{\tau_B} + \frac{1}{\tau_{\text{ph-e}}}. \tag{21}$$

The relaxation time for Umklapp scattering at high temperature (room and above), which is of interest here, was given by Klemens as<sup>14</sup>

$$\frac{1}{\tau_U} = 2\gamma^2 \frac{k_B T}{\mu V_0} \frac{\omega^2}{\omega_D}, \tag{22}$$

where  $\gamma$  is the Gruneisen anharmonicity parameter,  $\mu$  is the shear modulus,  $V_0$  is the volume per atom, and  $\omega_D$  is the Debye frequency. The shear modulus in Eq. (22) is treated as a velocity dependent effective value calculated for a given geometry. A more accurate expression for Umklapp scattering has been given in Ref. 10. Mass-difference scattering is the scattering of phonons due to differences in mass. The relaxation rate for the mass-difference scattering is calculated using the following expression:

$$\frac{1}{\tau_M} = \frac{V_0 \Gamma \omega^4}{4\pi V^3}, \tag{23}$$

where  $\Gamma$  is the measure of the strength of the mass-difference scattering defined as

$$\Gamma = \sum_i f_i \left(1 - \frac{M_i}{\bar{M}}\right)^2. \tag{24}$$

Here  $f_i$  is the fractional concentration of the impurity atoms of mass  $M_i$  and  $\bar{M} = \sum_i f_i M_i$  is the average atomic mass. One should notice that the phonon group velocity  $V$  is a function of the size of the low-dimensional structure and depends on the particular type of boundaries.<sup>10</sup>

For the consistency of the model, we modify the expression for the boundary scattering relaxation via introduction of parameter  $p$  to the semiempirical formula

$$\frac{1}{\tau_B} = \frac{V}{D} (1-p). \tag{25}$$

One can see that when  $p = 1$ , e.g., in the case of purely specular scattering, boundary scattering does not contribute

to the thermal resistivity. In the case of purely diffuse scattering,  $p=0$ , Eq. (25) reduces to the well-known Casimir limit<sup>15</sup>

$$\frac{1}{\tau_B} = \frac{V}{D}. \quad (26)$$

At low doping levels, the relaxation time for acoustic phonons scattered by electrons can be expressed as<sup>16</sup>

$$\frac{1}{\tau_{ph-e}} = \frac{n_e \epsilon_1^2 \omega}{\rho V^2 k_B T} \sqrt{\frac{\pi m^* V^2}{2 k_B T}} \exp\left(-\frac{m^* V^2}{2 k_B T}\right), \quad (27)$$

where  $n_e$  is the concentration of conduction electrons,  $\epsilon_1$  is the deformation potential,  $\rho$  is the mass density, and  $m^*$  is the electron effective mass. Here we assume that phonon confinement does not strongly affect phonon-electron scattering rates.<sup>17</sup>

### D. Phonon dispersions and phonon group velocities

We consider a generic cylindrical quantum wire along the  $z$  axis and assume that the main contribution to heat transfer along the wire comes from the longitudinal acoustic phonon modes. Following the approach of Refs. 18–20, the dispersion relations for phonons in a free-standing quantum wire with diameter  $D$  are given by

$$\begin{aligned} (q^2 - q_t^2)^2 \frac{(q_d D/2) J_0(q_d D/2)}{J_1(q_d D/2)} - 2q_d^2 (q^2 + q_t^2) \\ + 4q^2 q_d^2 \frac{(q_t D/2) J_0(q_t D/2)}{J_1(q_t D/2)} = 0, \end{aligned} \quad (28)$$

where  $q$  is the  $z$  component of the phonon wave vector,  $J_0$  and  $J_1$  are the ordinary Bessel functions, and  $q_d$  and  $q_t$  are two parameters related by

$$q_{d,t}^2 = \frac{\omega^2}{v_{d,t}^2} - q^2. \quad (29)$$

Here  $v_d = \sqrt{(\lambda + 2\mu)/\rho}$  and  $v_t = \sqrt{\mu/\rho}$  are the velocities of the longitudinal and transverse acoustic waves in bulk semiconductors, where  $\lambda$  and  $\mu$  are the Lamé constants, and  $\rho$  is the density. Phonon dispersions can be obtained by numerically solving Eqs. (28) and (29). At each  $q$ , there are many solutions for  $q_d$  and  $q_t$ . Using index  $n$  to indicate different solutions, we can write the phonon dispersion relations as

$$\omega_n = v_{d,t} \sqrt{q^2 + q_{d,t}^2}, \quad (30)$$

where  $\omega_n$  is the phonon frequency for the  $n$ th branch. By numerical differentiation, we obtain phonon group velocity for each branch

$$V_n = \frac{d\omega_n}{dq}. \quad (31)$$

In order to calculate the phonon thermal conductivity, we need to find the functional dependence of the phonon group velocity on phonon energy. Moreover, since different branches have different group velocity-energy dependencies, we have to calculate the phonon group velocity averaged over all contributing branches. The velocity average is weighted by the phonon population factor

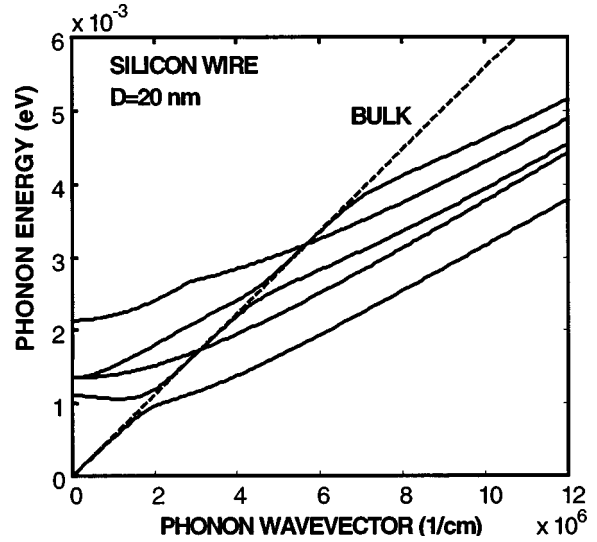


FIG. 1. Acoustic phonon dispersion relation for five lowest confined branches in a free-standing silicon cylindrical nanowire with a diameter of 20 nm. One can see that slope of the phonon branches, and thus the group velocities, are lower than those in the bulk.

$$\bar{V}(\hbar\omega) \equiv \frac{\sum_n V_n(\hbar\omega) \frac{N_n}{\sum_m N_m}}{\sum_n V_n(\hbar\omega) \frac{e^{\hbar\omega/k_B T}}{\sum_m e^{\hbar\omega/k_B T}}} \quad (32)$$

Equation (32) gives an approximate solution since the energy spacing between different branches is nonequidistant. The obtained  $\bar{V}(\hbar\omega)$  is then used to calculate the lattice thermal conductivity  $\kappa_l^{\text{wire}}$ .

### III. RESULTS OF SIMULATION AND DISCUSSION

First, we find the dispersion relations of confined acoustic phonon modes in a free-standing cylindrical quantum wire with a particular diameter by numerically solving Eqs. (28) and (29). Figure 1 shows the dispersion relations of the five lowest confined acoustic phonon branches in a silicon cylindrical nanowire with a diameter of 20 nm. The material parameters used in the simulation are  $v_d = 8.47 \times 10^5$  cm/s and  $v_t = 5.34 \times 10^5$  cm/s. In Fig. 1, one can see that only the first branch has a linear dispersion relation for very small values of  $q$ , and  $\omega = 0$  when  $q = 0$ . For the second branch and above, there exists a cut-off frequency, i.e.,  $\omega \neq 0$  when  $q = 0$ . The slope of the phonon branches, and thus the group velocities are lower than those in the bulk.

We find the exact values of the group velocity for each phonon branch by numerical differentiation. The group velocity for the first branch almost coincides with the bulk velocity for very small values of the phonon energy. It then drops dramatically with increasing energy and rises up again much more slowly and finally asymptotically reaches a constant value. Moreover, there are very sharp jumps and drops of the velocity for the second and above branches as can be expected from the phonon dispersion shown in Fig. 1. Averaging over all contributing phonon branches using the method described in part D of Sec. II, we find the average phonon group velocity as a function of the phonon energy. The population averaged group velocity is shown in Fig. 2. The overall value of the average phonon group velocity is

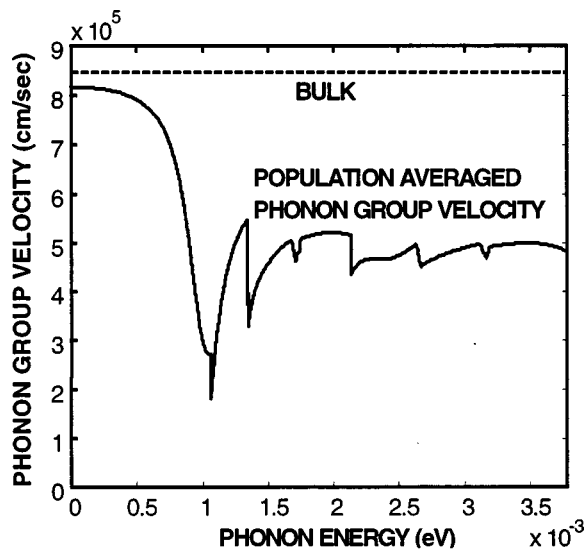


FIG. 2. Population averaged group velocity as a function of phonon energy. The overall value of the average phonon group velocity is  $5.39 \times 10^5$  cm/s, which is about half of the phonon group velocity in the bulk.

$5.39 \times 10^5$  cm/s, about half of the phonon group velocity in the bulk. In silicon, the longitudinal sound velocity in the bulk is  $8.47 \times 10^5$  cm/s. The average group velocity coincides with the first branch for small values of the phonon energy (up to 1 meV only). For higher values of the phonon energy, it oscillates about a constant value, which asymptotically reaches  $4.5 \times 10^5$  cm/s. One should remember that these values are obtained for specific geometry, size, and boundary conditions, and will be different in other structures.

Once the functional dependence of phonon group velocity on energy in a nanowire is found, we calculate phonon relaxation rates using Eqs. (22)–(27). Figure 3 shows the

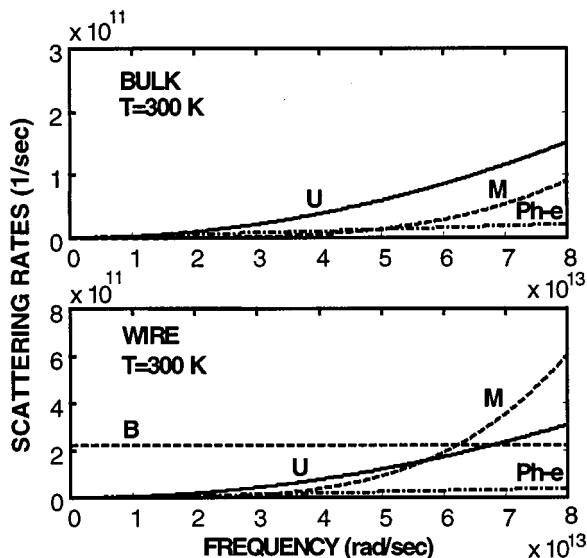


FIG. 3. Phonon scattering rates in a silicon nanowire of diameter  $D = 20$  nm due to different scattering mechanisms as functions of the phonon frequency. The results are shown for the three-phonon Umklapp, mass-difference, phonon-electron, and boundary scattering at  $T = 300$  K.

scattering rates for the three-phonon Umklapp, mass-difference, boundary, and phonon-electron scattering at 300 K both in the bulk and in the wire. The following material parameters have been used in the simulation:  $m^* = 0.26m_0$ , where  $m_0$  is the free electron mass,  $\rho = 2330$  kg/m<sup>3</sup>,  $\epsilon_1 = 9.5$  eV, and  $\Gamma = 8.357 \times 10^{-4}$ . The shear modulus is estimated from the formula  $\mu = v_t^2 \rho$  [see Eq. (29)]. In the bulk, Umklapp scattering dominates over mass-difference and phonon-electron scattering. The same is true for the quantum wells examined in Ref. 10. In our simulation, we considered semiconductors with a relatively low carrier concentration of  $10^{18}$  cm<sup>-3</sup>. The scattering rate for phonon-electron scattering at room temperature is small compared to that for Umklapp and mass-difference scattering. Thus, in lightly doped semiconductors, the phonon-electron scattering does not have a strong influence on the lattice thermal conductivity. However, for higher carrier concentrations, phonon-electron scattering becomes important, reaching the level of other relaxation mechanisms.

In a nanowire, boundary scattering is significant for the entire frequency range important for silicon. The latter is different from the quantum wells of comparable dimensions where mass-difference dominates over most of the large portion of the frequency range.<sup>10</sup> Mass-difference scattering in nanowires strongly increases at phonon frequency of about  $5 \times 10^{13}$  rad/s due to the inverse-cubic dependence of the relaxation rate on the phonon group velocity, which drops at this point to about 50% of its bulk value. Using obtained phonon group velocity and relaxation times, we calculate the lattice thermal conductivity in the wire, and compare the result with the bulk value.

After the group velocity is found, we calculate  $\kappa_l$  for a temperature range of 300–800 K from Eq. (12), which takes into account confined phonon dispersion in the wire. This gives us the lattice thermal conductivity  $\kappa_l$  in the framework of approach A1, which includes the decrease of the phonon group velocity in low-dimensional structures but does not account for the modification of nonequilibrium phonon distribution due to partially diffuse and partially specular interface scattering. Figure 4 shows the lattice thermal conductivity calculated using approach A1 in a cylindrical nanowire and bulk silicon. One can see that according to this model the lattice thermal conductivity in the wire is reduced to about 26% of its bulk value at 300 K. It is important to note that this result is obtained for idealized boundary conditions (free surface) with complete phonon confinement. Most of the practical situations fall into the category of mixed boundary conditions with partial phonon wave penetration through the boundaries. Quantitatively, the difference in the rigidity of materials that make up the boundary for acoustic phonons can be characterized by the acoustic impedance mismatch  $\zeta = \rho_w v_w / \rho_b v_b$ , where  $\rho_w$  ( $\rho_b$ ) is the density of the wire (barrier) material and  $v_w$  ( $v_b$ ) is the sound velocity in the wire (barrier) material. Even similar materials may have rather large acoustic mismatch  $\zeta$ . For example, the mismatch between Si and Ge calculated for longitudinal and transverse sound velocities is 0.75 and 0.71, respectively.<sup>3</sup> Thus, in a real nanowire embedded within material of different crystalline properties the actual drop of  $\kappa_l$  due to acoustic phonon

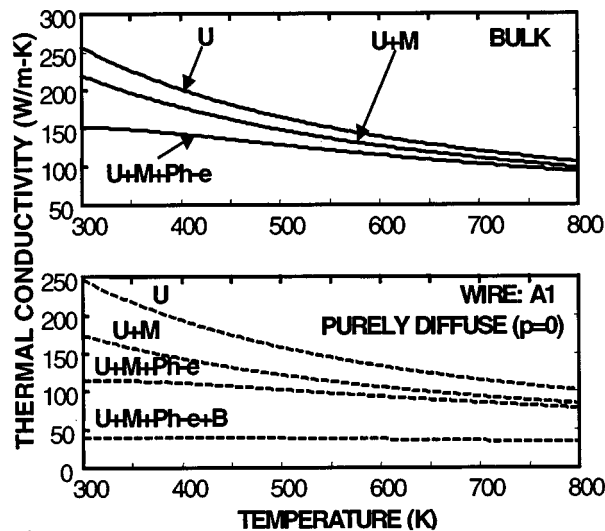


FIG. 4. Lattice thermal conductivity calculated using approach A1 in a cylindrical nanowire and bulk silicon. The results for the nanowire are calculated for the case of purely diffuse boundary scattering ( $p=0$ ). One can see that according to this model the lattice thermal conductivity in the wire is reduced to about 26% of its bulk value at 300 K. It is important to note that this value is obtained for the idealized boundary conditions (free surface) with complete phonon confinement.

confinement can be smaller owing to partial confinement of acoustic phonons.

To develop a self-consistent model we combine approaches A1 and A2, and introduce a correction  $\Delta\kappa_l^{\text{wire}}$  to  $\kappa_l$  in order to account for the deviation of nonequilibrium phonon distribution from its bulk form due to partially specular and diffuse interface scattering. We calculate  $\Delta\kappa_l^{\text{wire}}$  taking into account confined phonon dispersion and the corresponding phonon group velocity. Thus, we obtain a self-consistent expression for the lattice thermal conductivity  $\kappa_l^{\text{wire}}$ , which combines important features of both approaches A1 and A2. The results of the simulation are shown in Figs. 5, 6 and 7. Details of the derivation procedure and computer simulation are given in Ref. 21.

Figure 5 shows the lattice thermal conductivity as a function of temperature calculated on the basis of our model (denoted by A1+A2) and approach A1. For this plot we assumed purely diffuse phonon boundary scattering (Casimir limit). The flattening of the conductivity curve near room temperature is due to the addition of phonon-electron scattering. The electron density concentration used in the simulation is  $10^{18} \text{ cm}^{-3}$ , which is far beyond the intrinsic carrier concentration in silicon although it is still lower than the degenerate limit. One can see that inclusion of phonon redistribution effects together with phonon confinement leads to further decrease of the lattice thermal conductivity.

Figure 6 shows the lattice thermal conductivity at room temperature as a function of specular phonon-boundary scattering fraction  $p$ . In the figure, we show the results for the bulk, and those for the wire obtained using our self-consistent approach (A1+A2) and approach A1. One can see that for the purely diffuse boundary scattering, e.g.,  $p=0$ , the A1 model predicts that the lattice thermal conductivity drops in the wire to about 26% of the bulk value; while

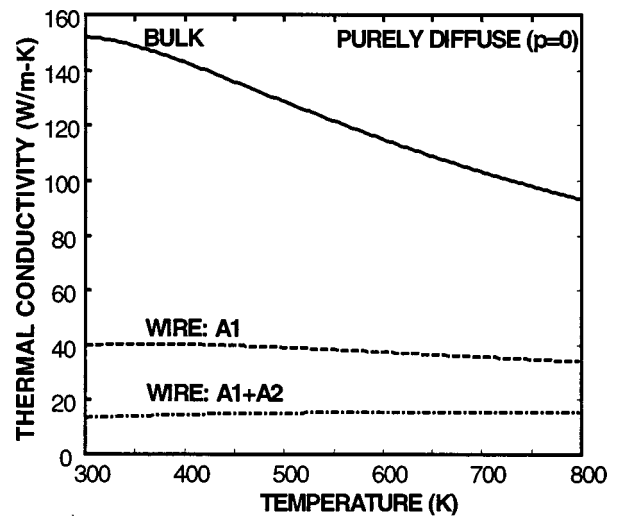


FIG. 5. Lattice thermal conductivity as a function of temperature for a silicon nanowire of diameter  $D=20 \text{ nm}$  calculated on the basis of our model (A1+A2) and approach A1. The results are shown for the case of purely diffuse scattering ( $p=0$ ).

our model (A1+A2) predicts further reduction to 9% of the bulk value. All the values are given for room temperature. In the purely specular boundary scattering case, e.g.,  $p=1$ ,  $\Delta\kappa_l^{\text{wire}}$  correction vanishes and our model coincides with A1. It is important to note that unlike model A2, in our approach the *bulk value is not recovered* for the case of purely specular scattering. This is a significant difference, important for heat transport simulation in deep submicron devices. The origin of this difference lies in the fact that our model takes into account modification of acoustic phonon dispersion in a quantum wire, which is present even if the wire has perfect boundaries and phonon boundary scattering is completely specular. The prediction of our model for the  $p=1$  case

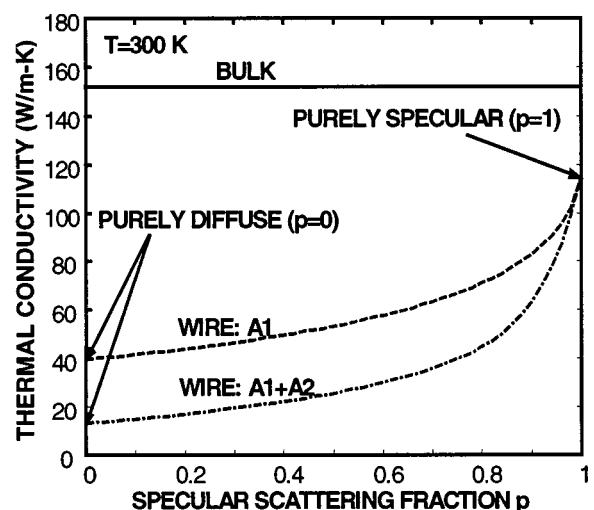


FIG. 6. Lattice thermal conductivity at room temperature as a function of specular phonon-boundary scattering fraction  $p$ . The results are shown for bulk and the wire of diameter 20 nm calculated based on our approach (A1+A2) and approach A1.

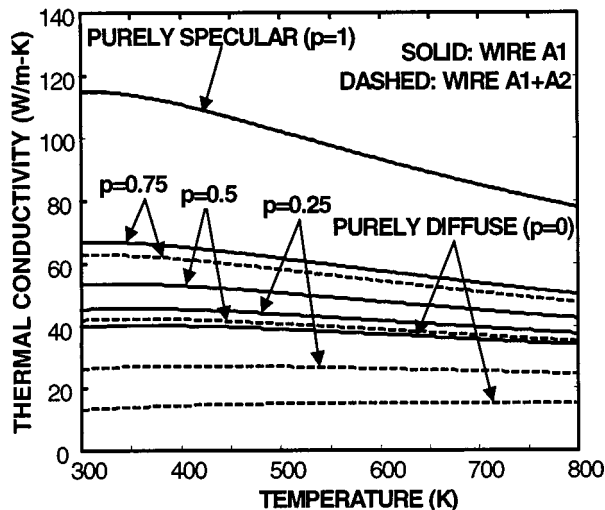


FIG. 7. Lattice thermal conductivity of a silicon nanowire as a function of temperature for different values of the specular phonon-boundary scattering fraction  $p$ . The results are shown for our model (A1+A2) and approach A1. One can see that our model (A1+A2) converges with approach A1 in the case of purely specular boundary scattering ( $p=1$ ).

(dominant specular boundary scattering) that the thermal conductivity is still below its bulk value is in agreement with experimental data reported to date.<sup>1,3,22</sup>

Figure 7 shows the lattice thermal conductivity as a function of temperature for different values of the specular phonon-boundary scattering fraction  $p$ . The results are shown for our model (A1+A2) and approach A1. One can see that for purely specular boundary scattering, e.g.,  $p=1$ , our approach (A1+A2) and approach A1 converge due to the fact that the correction  $\Delta\kappa_l^{\text{wire}}$  disappears in this case. However, for partially diffusive scattering our model (A1+A2) predicts a lower value of the lattice thermal conductivity than that obtained from approach A1. In particular, for purely diffusive boundary scattering, e.g.,  $p=0$ , our model (A1+A2) predicts a drop of the lattice thermal conductivity to about 9% of its bulk value while approach A1 predicts a reduction to about 26% of the bulk value. These values are obtained for the free-standing quantum wire.

#### IV. CONCLUSION

We have proposed a self-consistent model for calculating the lattice thermal conductivity in a semiconductor nanowire with lateral dimensions comparable to the phonon mean free path. The model takes into account both modifications of phonon dispersions due to spatial confinement and

change in nonequilibrium phonon distribution due to boundary scattering. All important phonon relaxation mechanisms such as three-phonon Umklapp scattering, mass-difference scattering, boundary scattering, and phonon-electron scattering are included into consideration. Phonon confinement and boundary scattering lead to a significant decrease of the lattice thermal conductivity. We show that inclusion of phonon confinement effects leads to deviation of the thermal conductivity from its bulk value even in the case of purely specular boundary scattering. This is an important observation that has to be taken into account in the simulation of heat transport in deep submicron and nanoscale devices.

#### ACKNOWLEDGMENT

The work was supported in part by the Semiconductor Research Corporation SRC Grant No. 99-NJ-741G (Dr. H. Hosack) and UC Energy Institute's EST program (Dr. S. Borenstein).

- <sup>1</sup>G. Chen, *Int. J. Therm. Sci.* **39**, 471 (2000).
- <sup>2</sup>K. E. Goodson and Y. S. Ju, *Annu. Rev. Mater. Sci.* **29**, 261 (1999).
- <sup>3</sup>A. Balandin, *Phys. Low-Dimens. Struct.* **1/2**, 1 (2000).
- <sup>4</sup>International Technology Roadmap for Semiconductor Industry, 1999.
- <sup>5</sup>D. Yang and J. B. Khurgin, *Superlattices Microstruct.* **27**, 245 (2000); S. Bandyopadhyay, A. Svizhenko, and M. A. Stroscio, *ibid.* **27**, 67 (2000).
- <sup>6</sup>T. G. Kim, X.-L. Wang, Y. Suzuki, K. Komori, and M. Ogura, *IEEE J. Sel. Top. Quantum Electron.* **6**, 511 (2000).
- <sup>7</sup>X. Sun, Z. Zhang, and M. S. Dresselhaus, *Appl. Phys. Lett.* **74**, 4005 (1999); A. Khitun, A. Balandin, K. L. Wang, and G. Chen, *Physica E (Amsterdam)* **8**, 13 (2000).
- <sup>8</sup>S.-W. Chung, J.-Y. Yu, and J. R. Heath, *Appl. Phys. Lett.* **76**, 2068 (2000).
- <sup>9</sup>A. Forchel, P. Ils, K. H. Wang, and O. Schilling, *Microelectron. Eng.* **32**, 317 (1996).
- <sup>10</sup>A. Balandin and K. L. Wang, *Phys. Rev. B* **58**, 1544 (1998).
- <sup>11</sup>A. Khitun, A. Balandin, and K. L. Wang, *Superlattices Microstruct.* **26**, 181 (1999).
- <sup>12</sup>S. G. Walskus, D. A. Broido, K. Kempa, and T. L. Reinecke, *J. Appl. Phys.* **85**, 2579 (1999).
- <sup>13</sup>S. G. Volz and G. Chen, *Appl. Phys. Lett.* **75**, 2056 (1999); S. G. Volz and D. Lemonnier, *Phys. Low-Dimens. Struct.* **5/6**, 91 (2000).
- <sup>14</sup>P. G. Klemens, in *Solid State Physics*, edited by F. Seitz and D. Turnbull (Academic, New York, 1958), Vol. 7, p. 1; P. G. Klemens, in *Chem. and Phys. of Nanostructures and Related Non-Equilibrium Materials*, edited by E. Ma, B. Fultz, R. Shall, J. Morral, and P. Nash (Minerals, Metals, & Materials Society, Warrendale, PA, 1997), p. 97.
- <sup>15</sup>H. B. G. Casimir, *Physica (Amsterdam)* **5**, 495 (1938).
- <sup>16</sup>J. E. Parrott, *Rev. Int. Hautes Temp. Refract.* **16**, 393 (1979).
- <sup>17</sup>N. Nishiguchi, *Phys. Rev. B* **54**, 1494 (1996).
- <sup>18</sup>N. Bannov, V. Aristov, and V. Mitin, *Phys. Rev. B* **51**, 9930 (1995).
- <sup>19</sup>SeGi Yu, K. W. Kim, M. A. Stroscio, and G. J. Iafrate, *Phys. Rev. B* **51**, 4695 (1995).
- <sup>20</sup>A. Svizhenko, A. Balandin, S. Bandyopadhyay, and M. A. Stroscio, *Phys. Rev. B* **57**, 4687 (1998).
- <sup>21</sup>J. Zou, Ph.D. thesis, University of California-Riverside (unpublished).
- <sup>22</sup>J. L. Liu, A. Balandin, T. Borca-Tascius, Y. S. Tang, K. L. Wang, and G. Chen, *Mater. Res. Soc. Symp. Proc.* **545**, 111 (1998).